JOURNAL OF MAGNETIC RESONANCE, Series A 109, 129–133 (1994)

Enhanced-Sensitivity Triple-Resonance Spectroscopy with Minimal H_2O Saturation

LEWIS E. KAY, GUANG YI XU, AND TOSHIO YAMAZAKI

Protein Engineering Network Centres of Excellence and Departments of Medical Genetics, Biochemistry, and Chemistry, Medical Sciences Building, University of Toronto, Toronto, Ontario, Canada M5S 1A8

Received February 21, 1994

Over the past few years several important advances in NMR have occurred which have contributed to the recording of spectra with increased sensitivity. These advances are the result of a number of factors including (i) the development of higher magnetic field strengths for commercial applications and increased stability electronics and (ii) the design of new pulse schemes which offer significant improvements in signal-to-noise. An example in this latter category includes the enhanced-sensitivity experiments developed by Cavanagh, Palmer, and Rance (*1–4*). These experiments, in the case of 2D NMR applications, for example, preserve both cosine- and sine-modulated t_1 frequency components so that a net gain in signal-to-noise of as much as a factor of $\sqrt{2}$ can be realized. Recently our laboratory (*5–7*) and others (*8*) have incorporated the enhanced-sensitivity method into heteronuclear, multidimensional experiments which make use of pulsed field gradients to discriminate between N- and P-type coherence-transfer pathways and have shown that sensitivity enhancements can be realized in these experiments as well.

An alternative approach for improving the sensitivity of a large class of experiments recorded in H_2O has recently been proposed by Grzesiek and Bax (*9, 10*). These workers note that because the T_1 of bulk H_2O can often be considerably longer than the ^1H T_1 values in proteins and that since for signal-to-noise reasons the repetition rate per scan must be faster than the relaxation rate of bulk water, partial saturation of water occurs in many NMR experiments, even if water suppression techniques such as presaturation are avoided. Partial saturation of water magnetization leads to an overall decrease in the intensity of protein resonances due to saturation transfer arising from chemical exchange involving labile protons and/or cross relaxation. Grzesiek and Bax stress the importance of minimizing saturation/dephasing of water magnetization during the course of the pulse sequence and suggest, therefore, that the water magnetization be restored to the $+z$ axis before acquisition in each scan. Montelione and co-workers have also demonstrated decreases in signal-to-noise ratios in ^1H–^{15}N HSQC spectra as a function of increasing exchange with water and decreasing relaxation delays (*11*). In this Communication, we demonstrate an enhanced-sensitivity HNCO experiment (i) which incorporates pulsed field gradients to select for the coherence-transfer pathway involving ^{15}N and makes use of the "enhanced-sensitivity approach" described by Rance and co-workers (*1, 4*) and (ii) which minimizes the degree of water saturation during the course of the pulse sequence (*9, 10*). For the cellulose-binding-domain fragment of a cellulase from *Cellulomonas fimi* (CBD), a dimer consisting of 110 amino acid monomers, an average sensitivity increase of approximately 35% over the previously published enhanced-sensitivity HNCO experiment is obtained (*7*).

Figure 1 illustrates the pulse scheme employed to obtain enhanced-sensitivity HNCO spectra with gradients to select for the coherence-transfer pathway passing through nitrogen and where saturation of the water magnetization is minimized. The mechanism of magnetization transfer in this sequence, including the sensitivity gains that can be expected for protein applications as a result of refocusing both cosine- and sine-modulated ^{15}N magnetization components, has been described in detail previously (*7*) and will not be repeated herein. Rather we focus attention on the approach used to ensure that saturation of water magnetization is kept to a minimum. Magnetization originates on the NH proton and is transferred via an INEPT sequence (*12*) to the one-bond-coupled ^{15}N spin. At point a in the sequence the magnetization of interest is of the form I_zN_z, where I_z and N_z correspond to the longitudinal components of amide proton and nitrogen magnetization, respectively. In many sequences (including most of our own!) a gradient is applied at this point. Insertion of a gradient at this point in the sequence has no effect on the desired signal (I_zN_z) but does eliminate any potential artifacts arising from signals in the transverse plane (*13*). In addition, because water magnetization is also in the transverse plane, it can be effectively dephased. While the use of gradients to dephase water does aid significantly in water suppression, it does so at a price. The intensity of labile protein protons decreases due to chemical exchange with dephased water protons, leading to a decrease in the overall envelope of the protein due to saturation transfer,

1064-1858/94 $6.00

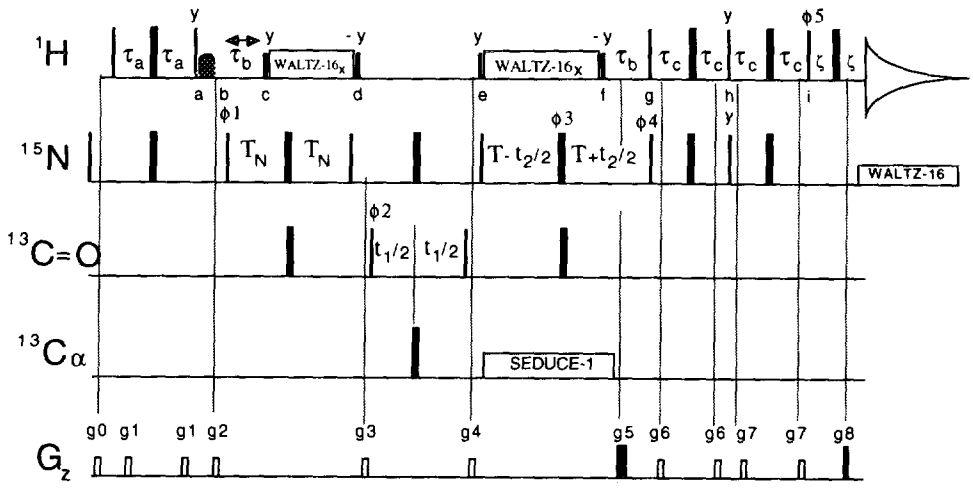

FIG. 1. Pulse scheme for the enhanced-sensitivity HNCO experiment using pulsed field gradients to select for the coherence-transfer pathway involving ^{15}N magnetization and employing a "water-selective pulse" to ensure that saturation of water is minimized. All narrow (wide) pulses have a flip angle of 90° (180°). All proton pulses are centered on the water resonance and are applied with a field of 23.8 kHz, with the exception of the 6.7 kHz $90°_{y/-y}$ pulses on either side of the WALTZ-16 decoupling field (*14*) and the water-selective pulse. The selective water pulse is either a 2 ms 90° rectangular pulse (125 Hz field) or a 2 ms shaped pulse having the profile of a 90° SEDUCE-1 element (*19*). ^{1}H decoupling is achieved using a 6.7 kHz WALTZ-16 decoupling field (*14*) with pulses applied along the $+x/-x$ axes while ^{15}N decoupling during acquisition employs a 1 kHz WALTZ field. The carbonyl pulses are applied using a field strength of 3.8 kHz; the ^{13}Cα 180° pulse is applied as a phase-modulated pulse (*20, 21*) with an excitation maximum at 58 ppm using a field of 8.5 kHz. A SEDUCE-1 decoupling field (*19, 22*) (320 μs 90° pulses; 1.7 kHz field at peak height) is employed to eliminate evolution due to the ^{15}N–^{13}Cα scalar coupling interaction during the constant-time ^{15}N evolution period. The SEDUCE-1 decoupling scheme is terminated 2.5 ms prior to point g in the sequence to allow for the application of gradient g5. The evolution due to the ^{15}N–^{13}Cα scalar coupling during this 2.5 ms period is small. The delays used in the sequence are $\tau_a = \tau_c = 2.3$ ms, $\tau_b = 5.5$ ms, $T_N = T = 12.4$ ms, and $\zeta = 0.5$ ms. The phase cycle employed is $\phi_1 = x, -x$; $\phi_2 = 4(x), 4(-x)$; $\phi_3 = 2(x), 2(-x)$; $\phi_4 = x$; $\phi_5 = x$; Acq $= 2(x, -x), 2(-x, x)$. The delays and strengths of the gradients are g0 = (0.5 ms, 8 G/cm), g1 = (0.5 ms, 5 G/cm), g2 = (2 ms, 15 G/cm), g3 = (0.75 ms, 20 G/cm), g4 = (0.2 ms, 5 G/cm), g5 = (1.25 ms, 30 G/cm), g6 = (0.3 ms, 5 G/cm), g7 = (0.2 ms, 10 G/cm), g8 = (0.125 ms, 27.8 G/cm). For each value of t_2, N- and P-type coherences are obtained by recording data sets where the sign of g5 is reversed and the phase of ϕ_4 inverted. Data obtained for positive and negative g5 values are stored in separate memory locations. Postacquisition processing of the data generates a pure-absorption data set by adding and subtracting N- and P-type signals, storing these results in separate memory locations, and applying a 90° zero-order phase correction to either the sum or the difference data (but not both). Quadrature in t_1 (carbonyl dimension) is obtained by States–TPPI of ϕ_2 (*23*).

while cross relaxation with proximate water molecules results in a further attenuation of protein signals.

The selective ^{1}H pulse applied at a in Fig. 1 restores the water magnetization to the $+z$ axis prior to the application of gradient g2 at point b, while minimizing the perturbation of NH magnetization aligned along the z axis at this time. Note that gradient g2 can still eliminate potential artifacts arising from transverse signals. Application of the ^{15}N pulse of phase ϕ_1 establishes antiphase nitrogen magnetization which subsequently refocuses during the delay $\tau_b = 1/(2J_{NH})$. The ^{1}H 90° pulse applied at point c in the sequence does not affect the desired signal; however, the water magnetization which was previously located on the $+z$ axis is rotated so as to be colinear with the subsequent WALTZ-16 decoupling field (*14*). As noted previously in the literature (*15–17*), the application of coherent proton decoupling at this point ensures that nitrogen magnetization does not evolve due to the one-bond ^{1}H–^{15}N scalar coupling, thereby increasing the effective relaxation time of the nitrogen signal. Water magnetization remains locked along the x axis during the decoupling with relaxation occurring at a rate given by the $T_{1\rho}$ of water. For small molecules tumbling in the extreme-narrowing regime, $T_{1\rho}$ relaxation is extremely inefficient over time periods such as between points c and d or e and f in Fig. 1 (~20 ms). Water magnetization is subsequently restored to the $+z$ axis at point d in the sequence through the application of a $90°_{-y}$ pulse. Note that, at this point in the sequence, the desired magnetization is of the form N_zC_z, where C_z is the z component of carbonyl magnetization, and the ^{1}H 90° pulse at point d has no effect on this component.

If the $+y$ and $-y$ ^{1}H pulses were omitted at positions c and d, respectively, the effect of the WALTZ-16 (*14*) decoupling field with pulses applied along the $+x/-x$ axes would be to result in a net rotation of water magnetization in the y–z plane (*15*). Even in the limit of perfect RF homogeneity and neglecting radiation damping, only an integral number of decoupling cycles will restore the water to the $+z$ axis. Positioning of the water signal along the decoupling field ensures that after ^{1}H decoupling the position of the water magnetization is known so that it can be restored efficiently to the $+z$ axis. Gradient pulses g3 and g4 are applied

when the magnetization of interest is of the form N_zC_z and when water magnetization is along the $+z$ axis. Any transverse magnetization (including water not along the z axis) is dephased by these gradient pulses. Carbonyl chemical shift is recorded during the t_1 period and magnetization subsequently transferred back to ^{15}N, with nitrogen chemical-shift evolution occurring during the ensuing $2T$ constant-time delay. Water magnetization is flipped to the x axis by the 90°_y ^1H pulse at point e in the sequence and remains spin locked until point f, at which time the magnetization is restored to the $+z$ axis. Therefore, application of gradient g5, which in concert with gradient g8 enables N-type or P-type coherence-transfer selection of ^{15}N signals (*5–7*), does not dephase the water. However, any water not aligned along the z axis due to pulse imperfections or radiation damping is dephased at this time. During the τ_b period, ^{15}N magnetization evolves due to the ^1H–^{15}N scalar coupling. At point g in the sequence simultaneous ^{15}N and ^1H pulses are applied, marking the start of the transfer of magnetization back to the amide proton for detection.

The back transfer is more complex than in unenhanced versions of the experiment (*18*) since both cosine- and sine-modulated components of signal in t_2 are transferred into observable magnetization using this approach. For all proteins examined in our laboratory to date, ranging in molecular weight from ~10 to 37 kDa, this approach results in sensitivity gains. Immediately after the ^1H 90° pulse at g, H_2O magnetization is along the $-y$ axis. The subsequent τ_c 180° τ_c period results in a net rotation of this magnetization by 180° so that it lies along the y axis at point h. Any water magnetization which is displaced from the y axis as a result of imperfections associated with the ^1H 180° pulse is effectively dephased by the gradient pair g6. After point i in the sequence the water magnetization is aligned along the $-z$ axis and the subsequent 180°_x pulse in the middle of the ζ period returns the signal to the $+z$ axis prior to detection. Finally, depending on the relative phases of gradients g5 and g8, gradient g8 refocuses either N-type or P-type echoes and simultaneously eliminates any (small) residual water that may remain in the transverse plane.

In the preceding discussion it was assumed that the "water-selective" pulse (shaped pulse in Fig. 1) has no effect on the signal of interest. Of course, this is true only if the excitation profile of this pulse is such that there is no perturbation of NH magnetization. Because upfield-shifted NH peaks in spectra of proteins can resonate in the proximity of the water line in some cases, it is important that the selective pulse shape and duration be chosen with care so as to minimize excitation of NH magnetization. The excitation profiles as a function of chemical-shift offset in hertz (i.e., offset from water) for two 90° "selective" pulses, starting with magnetization along the $+z$ axis, are shown in Fig. 2. In particular, profiles for a 2 ms rectangular pulse (125 Hz field) and a 2 ms pulse having the shape of a SEDUCE-1 (*19*) 90° element

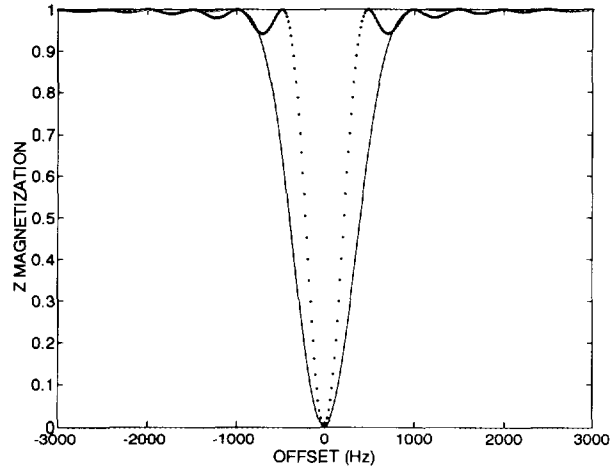

FIG. 2. Excitation profile of z magnetization due to a 90° 2 ms rectangular pulse (125 Hz) (·) and a 2 ms pulse (—) having the shape of a 90° SEDUCE-1 (*19*) element (272 Hz at peak height).

(272 Hz field at peak amplitude) are indicated. For NH shifts approximately 780 Hz downfield of water (≥6.3 ppm at 500 MHz), the SEDUCE-1 pulse is preferred over the rectangular pulse since the latter can (slightly) affect NH signals further downfield. On the other hand, the 2 ms rectangular pulse results in significantly less excitation of resonances in the vicinity of the water peak, so that upfield-shifted NH resonances (≤6.3 ppm) are less perturbed. In practice, we find that both pulses work equally well.

The key to maximizing the sensitivity gains in any experiment where water saturation is to be minimized is to know where the water signal is at all times during the sequence. It is important, therefore, that the effects of radiation damping be kept in mind. For example, consider a simple 90°—delay pulse sequence. After the 90° pulse, water magnetization is excited into the transverse plane; however, very quickly thereafter it is restored to the $+z$ axis by virtue of radiation damping. Figure 3 illustrates the decay of water magnetization in the transverse plane following a 90° excitation pulse. After ~50 ms the water has been completely restored to the z axis. In order to avoid the effects of radiation damping during the INEPT transfer delays in the present sequence, gradients are applied so as to dephase the water for the majority of the transfer time (e.g., g1, g6, and g7 in Fig. 1). Because both the delays and the gradients employed are relatively small, attenuation of the water signal due to diffusion is negligible.

In order to quantitate the sensitivity gains that can be realized by restoring water to the $+z$ axis prior to detection and by minimizing saturation/dephasing of water magnetization during the course of the pulse sequence, 2D (F_2,F_3) spectra were acquired with the sequence illustrated in Fig. 1. A sample of the cellulose binding domain of a cellulase from *C. fimi*, a protein fragment consisting of a dimer of

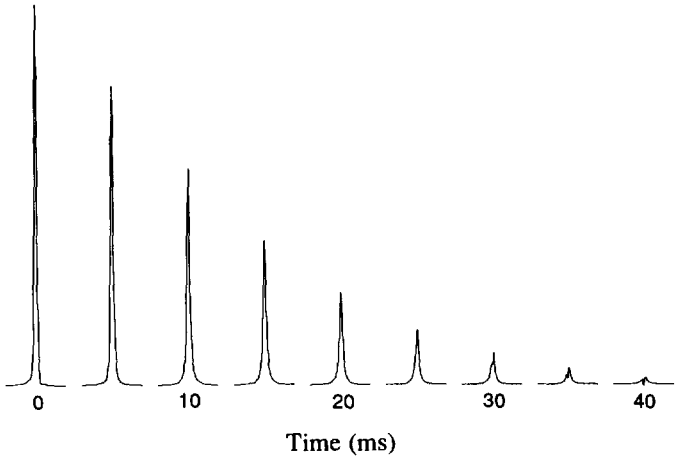

FIG. 3. Decay of water magnetization in the transverse plane after a 90° pulse. The pulse sequence used to measure the decay is 90°—delay—acquire. Delay values of 0 to 40 ms in increments of 5 ms are employed.

110 amino acid monomers, 1.5 mM, 90% H_2O, 10% D_2O, pH 7.0, 30°C was used. Spectra were recorded on a Varian UNITY-500 MHz spectrometer equipped with a triple-resonance probe with an actively shielded z gradient.

Figure 4 illustrates the normalized intensity ratios of cross peaks as a function of residue number for CBD. Two-dimensional ^{15}N–NH spectra were acquired with the sequence in Fig. 1 with t_1 set to zero, a carbonyl 180° pulse applied in the center of the t_1 evolution time, and the $^{13}C\alpha$ 180° pulse removed. Normalized cross-peak intensities were generated using the formula I_a^i/I_b^i, where I_a^i is the intensity of cross peak i in the experiment in Fig. 1 (Experiment a) and I_b^i is the intensity of the corresponding cross peak in experiment b, where the shaped pulse in experiment a is removed and in addition the $^1H_{y/-y}$ pulses flanking the WALTZ-16 decoupling periods (*14*) are eliminated. This sequence is essentially the enhanced-sensitivity scheme that we proposed previously (*7*). The relative intensities of cross peaks in spectra recorded with either a 2 ms rectangular pulse or a 2 ms pulse with the SEDUCE-1 (*19*) profile are illustrated in Fig. 4a. The differences in cross-peak intensities obtained with the two different selective pulses are very small.

In order to emphasize the importance of setting the water magnetization along the $+z$ axis prior to the detection period we have also investigated the signal intensities of cross peaks obtained in spectra generated by placing the water magnetization along the $-z$ axis prior to the acquisition period. This was achieved by adding 180° to the phase tables for ϕ_4 and ϕ_5. In this case a different steady state for the water magnetization occurs. We have determined experimentally that the sequence which places water magnetization along the $+z$ axis preserves ~65% of the equilibrium water magnetization while only 11% of the equilibrium magnetization remains in steady state (and with opposite phase) when the water is aligned along the $-z$ axis. The results of this experiment are illustrated in Fig. 4b, which shows normalized cross-peak intensities, I^i_{-a}/I^i_b, where I^i_{-a} is the intensity of cross peak i in the experiment in Fig. 1 with the exception that water magnetization is stored along the $-z$ axis. Clearly, the differences in intensity between cross peaks from the I_{-a} and I_a spectra are significant, suggesting that it is worthwhile

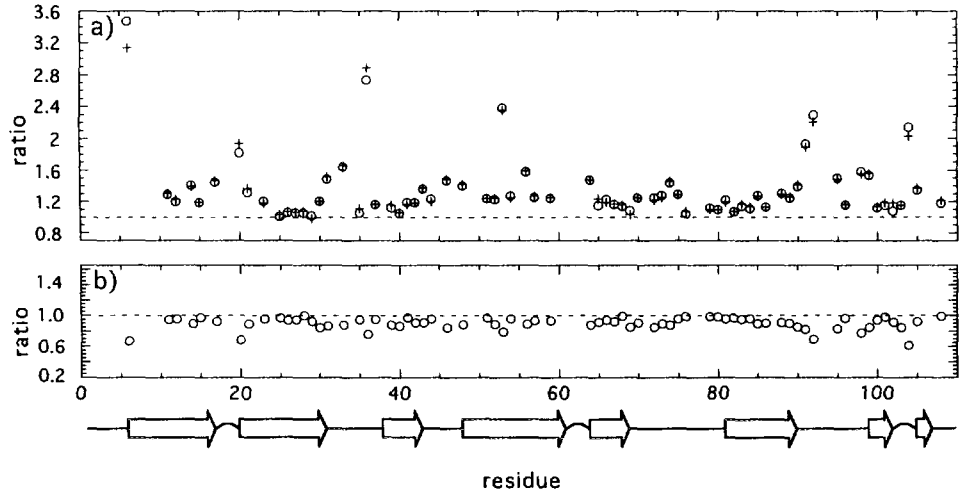

FIG. 4. (a) Relative cross-peak intensities obtained from the ratio of cross peaks generated using the experiment indicated in Fig. 1 vs cross peaks obtained from the experiment in Fig. 1 where the shaped pulse is removed and the ^1H $90^\circ_{y/-y}$ pulses flanking the WALTZ-16 (*14*) decoupling periods are eliminated. The intensities of cross peaks in spectra recorded with either a 2 ms rectangular pulse (+) or a 2 ms pulse with the SEDUCE-1 (*19*) profile (○) are illustrated. Average intensity gains of 1.36 are obtained for rectangular and SEDUCE-1 selective pulses. (b) Same as in (a) with the exception that 180° is added to the phase tables for ϕ_4 and ϕ_5, placing the water magnetization along the $-z$ axis; 2 ms SEDUCE-1 pulses are employed. An average intensity ratio of 0.90 is measured. The relaxation delay used in all experiments was 0.9 s. The secondary structure of this largely β-sheet protein is indicated.

to ensure that water magnetization is restored to the $+z$ axis prior to detection. In fact, averaged over all resolved cross peaks in the spectrum, an overall intensity gain of a factor of 1.36 (I^i_a/I^i_b) is obtained using either the SEDUCE or the rectangular selective pulse while an average gain of a factor of 1.22 is noted for the structured β-sheet regions of the protein. This is to be contrasted with a value for I^i_{-a}/I^i_b of 0.90.

In summary, in this Communication it has been shown that with a few minor modifications to the enhanced-sensitivity triple-resonance experiments that we have described previously (*7*), it is possible to minimize saturation of water magnetization during the course of the experiment. As Grzesiek and Bax have demonstrated previously (*9, 10*), sensitivity gains can be achieved using this approach. The extent of improvement in signal-to-noise will be a function of the protein studied and the sample conditions. For the case of CBD an overall average sensitivity gain of over a factor of two is obtained using the present enhanced-sensitivity pulse scheme relative to a nongradient unenhanced version which uses a 30 Hz presaturation field during the relaxation delay. For proteins which are only stable at pH values greater than 7.0 or where exchange with water is more prevalent than in the protein considered here, the gains in sensitivity may well be even larger.

ACKNOWLEDGMENTS

The authors thank Dr. Steve Smallcombe, Varian Inc., for valuable discussions and Drs. Warren, Kilburn, and Wong, University of British Columbia, for the gift of ^{15}N,^{13}C-labeled CBD.

REFERENCES

1. J. Cavanagh and M. Rance, *J. Magn. Reson.* **88,** 72 (1990).
2. A. G. Palmer, J. Cavanagh, P. E. Wright, and M. Rance, *J. Magn. Reson.* **93,** 151 (1991).
3. A. G. Palmer, J. Cavanagh, R. A. Byrd, and M. Rance, *J. Magn. Reson.* **96,** 416 (1992).
4. J. Cavanagh and M. Rance, *Annu. Rep. NMR Spectrosc.* **27,** 1 (1993).
5. L. E. Kay, P. Keifer, and T. Saarinen, *J. Am. Chem. Soc.* **114,** 10663 (1992).
6. D. R. Muhandiram, G. Y. Xu, and L. E. Kay, *J. Biomol. NMR* **3,** 463 (1993).
7. D. R. Muhandiram and L. E. Kay, *J. Magn. Reson. B* **103,** 203 (1994).
8. J. Schleucher, M. Sattler, and C. Griesinger, *Angew. Chem. Int. Ed. Engl.* **32,** 1489 (1993).
9. S. Grzesiek and A. Bax, *J. Biomol. NMR* **6,** 627 (1993).
10. S. Grzesiek and A. Bax, *J. Am. Chem. Soc.* **115,** 12593 (1993).
11. Y. Li and G. T. Montelione, *J. Magn. Reson. B* **101,** 315 (1993).
12. G. A. Morris and R. Freeman, *J. Am. Chem. Soc.* **101,** 760 (1979).
13. A. Bax and S. Pochapsky, *J. Magn. Reson.* **99,** 638 (1992).
14. A. J. Shaka, J. Keeler, T. Frenkiel, and R. Freeman, *J. Magn. Reson.* **52,** 335 (1983).
15. A. Bax, M. Ikura, L. E. Kay, D. A. Torchia, and R. Tschudin, *J. Magn. Reson.* **86,** 304 (1990).
16. R. E. London, *J. Magn. Reson.* **86,** 410 (1990).
17. J. W. Peng, V. Thanabal, and G. Wagner, *J. Magn. Reson.* **95,** 421 (1991).
18. S. Grzesiek and A. Bax, *J. Magn. Reson.* **96,** 432 (1992).
19. M. A. McCoy and L. Mueller, *J. Am. Chem. Soc.* **114,** 2108 (1992).
20. J. Boyd and N. Scoffe, *J. Magn. Reson.* **65,** 406 (1989).
21. S. L. Patt, *J. Magn. Reson.* **96,** 94, (1992).
22. M. A. McCoy and L. Mueller, *J. Magn. Reson.* **98,** 674 (1992).
23. D. Marion, M. Ikura, R. Tschudin, and A. Bax, *J. Magn. Reson.* **85,** 393 (1989).